The Last Common Ancestor of Most Bilaterian Animals Possessed at Least Nine Opsins

M. Desmond Ramirez[1,*], Autum N. Pairett[2], M. Sabrina Pankey[3], Jeanne M. Serb[2], Daniel I. Speiser[4], Andrew J. Swafford[1], and Todd H. Oakley[1,*]

[1]Department of Ecology, Evolution and Marine Biology, University of California, Santa Barbara, CA

[2]Department of Ecology, Evolution and Organismal Biology, Iowa State University, Ames, IA

[3]Department of Molecular, Cellular and Biomedical Sciences, University of New Hampshire, Durham, NH

[4]Department of Biological Sciences, University of South Carolina, Columbia, SC

*Corresponding authors: E-mails: mdesmondramirez@gmail.com; oakley@lifesci.ucsb.edu.

Abstract

The opsin gene family encodes key proteins animals use to sense light and has expanded dramatically as it originated early in animal evolution. Understanding the origins of opsin diversity can offer clues to how separate lineages of animals have repurposed different opsin paralogs for different light-detecting functions. However, the more we look for opsins outside of eyes and from additional animal phyla, the more opsins we uncover, suggesting we still do not know the true extent of opsin diversity, nor the ancestry of opsin diversity in animals. To estimate the number of opsin paralogs present in both the last common ancestor of the Nephrozoa (bilaterians excluding Xenoacoelomorpha), and the ancestor of Cnidaria + Bilateria, we reconstructed a reconciled opsin phylogeny using sequences from 14 animal phyla, especially the traditionally poorly-sampled echinoderms and molluscs. Our analysis strongly supports a repertoire of at least nine opsin paralogs in the bilaterian ancestor and at least four opsin paralogs in the last common ancestor of Cnidaria + Bilateria. Thus, the kernels of extant opsin diversity arose much earlier in animal history than previously known. Further, opsins likely duplicated and were lost many times, with different lineages of animals maintaining different repertoires of opsin paralogs. This phylogenetic information can inform hypotheses about the functions of different opsin paralogs and can be used to understand how and when opsins were incorporated into complex traits like eyes and extraocular sensors.

Key words: reconciled tree, eye evolution, extraocular photoreceptors, phototransduction, vision.

Introduction

As the protein component of visual pigments, opsins are used in the majority of light detectors found in animals (Nilsson 2013; Oakley and Speiser 2015). Opsins are G-protein coupled receptors which bind light-sensitive chromophores via Schiff base linkages at a conserved lysine residue (Terakita 2005). When the chromophore absorbs a photon, conformational changes in the chromophore and opsin protein activate G-protein signal transduction (Terakita 2005). Despite their widespread importance in animal photosensitivity, most work on the function and evolution of opsins focused initially on those expressed in the eyes of vertebrates and arthropods (Nathans and Hogness 1983; O'Tousa et al. 1985). Only more recently has work on opsins included those expressed outside eyes or from other animal phyla (Velarde et al. 2005; Radu et al. 2008; Hering et al. 2012; Hering and Mayer 2014; D'Aniello et al. 2015). We now know the evolutionary history of opsins is one of many gains and losses of genes across time and among species (Colbourne et al. 2011; Davies et al. 2015; Henze and Oakley 2015; Liegertová et al. 2015; Feuda et al. 2016). Understanding this kind of high gene turnover requires broad taxonomic sampling of opsins to fully reconstruct their evolutionary origins, especially because we know that ancient losses may result in the complete absence of some opsin paralogs, even in major groups of animals. Previous large-scale opsin phylogenies have also found many sequences that fall

outside of the well-known opsin groups, typically identified in taxa for which we have sparse data, for example arthropsins in *Daphnia* or Echinopsins B in echinoderms (Colbourne et al. 2011; D'Aniello et al. 2015). Most analyses do not address the nature of these orphaned sequences. While they may be recently diverged, lineage-specific duplications, another possibility is that they represent entire opsin paralogs that are absent from the phyla that have been most heavily sampled. Without an accurate picture of how opsin paralogs are distributed among animals, it is challenging to address how diverse opsins really are, when that diversity arose, and when and how different opsins were integrated into different kinds of light-detecting structures during evolution.

Opsins evolved very early in animals (Plachetzki et al. 2007; Feuda et al. 2012; Oakley and Speiser 2015), likely first expressed in light-sensitive cells and later in more complex structures like eyes (Arendt and Wittbrodt 2001; Nilsson 2013). Historically, opsin diversity has been partitioned among three clades: the "ciliary" or c-opsins, the "rhabdomeric" or r-opsins, and "Group 4 opsins" *sensu* Porter et al. (2012). We propose renaming the c- and r-opsin paralogs "canonical c-opsin" and "canonical r-opsin" to denote the originally described visual opsins of vertebrates and invertebrates (Terakita 2005). We also propose renaming the "Group 4 opsins" coined by Porter et al. (2012) as tetraopsins. Hereafter, we refer to these opsins by these new names. A possible fourth clade of opsins, cnidops, is currently known only from cnidarians and includes sequences from all major cnidarian classes (Plachetzki et al. 2007; Feuda et al. 2012). To understand how many opsin paralogs were present in the last common eumetazoan and bilaterian ancestors, we need to understand when these major opsin clades arose and how they are related to each other.

Because cnidarians represent a rare nonbilaterian animal lineage with opsins, their opsin repertoire provides key insights into the opsin paralogs present in the last common ancestor of eumetazoans. However, relating cnidarian opsins to the major animal opsin paralogs has proved difficult, and hypotheses on how cnidarian and bilaterian opsins relate vary widely between analyses. For example, some analyses indicate cnidarian genomes encode either cnidops alone (Porter et al. 2012; Liegertová et al. 2015), or cnidops plus canonical c-opsins (Plachetzki et al. 2007; Vopalensky and Kozmik 2009). However, others suggest the most recent ancestor of eumetazoans had three opsin paralogs: canonical c- and r-opsins, and tetraopsins (Suga et al. 2008; Feuda et al. 2012, 2014; Bielecki et al. 2014). Based on in vitro assays, an opsin (Acropsin 3) from the coral *Acropora palmata* interacts with the same G-protein q α subunit used by canonical r-opsins (Lee et al. 1994; Mason et al. 2012). Together with the hypothesized phylogenetic position of Acropsin 3, the functional test suggests that some cnidarians may possess canonical r-opsins (Mason et al. 2012). Still, the exact placement of this and other cnidarian opsins is highly sensitive to the specific

substitution models and gene sampling regimes used in each analysis.

Reconstructing opsin evolution in bilaterians poses yet more challenges. Early estimates of opsin diversity in the last common bilaterian ancestor identified two (canonical c- and r-opsins; Nilsson 2005) or three (canonical c-, r- and tetraopsins; Plachetzki et al. 2007; Feuda et al. 2012, 2014; Porter et al. 2012) paralogs. Recent sampling efforts to survey new taxa and extraocular tissues have expanded our current view of opsin diversity, and we now recognize that multiple clades of opsins found in extant animals were present in the last common ancestor of bilaterians, based on their presence in both deuterostome (e.g. vertebrates and echinoderms) and protostome (e.g. arthropods and molluscs) genomes. These considerations indicate at least five opsin paralogs in the last common ancestor of bilaterians (five: Terakita 2005; Suga et al. 2008; Vopalensky and Kozmik 2009; six: Feuda et al. 2014; Hering and Mayer 2014; Liegertová et al. 2015), distributed between the bilaterian c-, r- and tetraopsins. With these additions, a pattern emerges: as we catalog opsins in diverse phyla and from different types of light receptors, we uncover greater diversity of opsin paralogs. A further wrinkle is recent strong support for the hypothesis that Acoelomorpha and Xenoturbella together are sister (as Xenacoelomorpha) to other bilaterians (Cannon et al. 2016). This result requires including Xenacoelomorpha opsins in order to estimate the number of opsin paralogs in the last common ancestor of bilaterians. Because no analysis to date, ours included, considers Xenacoelomorpha opsins, at present we can only truly infer the opsin repertoire for the lsat common ancestor of Nephrozoa (Prostomia + Deuterostomia, excluding Xenacoelomorpha).

A primary goal of our analysis is to reconstruct a more taxonomically comprehensive evolutionary history of animal opsins to understand the origins of bilaterian opsin diversity. We achieve this in two ways. First, we include newly published opsin sequences from multiple studies that have yet to be synthesized in a large scale phylogenetic analysis. Second, we identify additional new opsins from both publicly available transcriptomes and nine unpublished mollusc transcriptomes, as molluscs are the second most speciose phylum but lag far behind other large taxa in terms of representation in opsin phylogenies to date. With this more comprehensive dataset, we produced the first large-scale formally reconciled opsin phylogeny and we use it to more explicitly estimate the number of opsins present in the last common ancestor of Protostomia + Deuterostomia. Tree reconciliation rearranges low-support branches to minimize the number of duplications and losses across the tree, which allows us to infer at least nine opsin paralogs were likely present in early bilaterians. Further, from the distribution of cnidarian opsins we infer that the last common ancestor of eumetazoans had at least four opsin paralogs. These results suggest a radiation in opsin diversity prior to the origin of bilaterians, followed by unique patterns

of duplications and losses specific to different animal lineages. Finally, these results urge a renewed focus on surveying opsins in understudied phyla (prime candidates include Annelida and Xenacoelomorpha, and nonbilaterians like Cnidaria and Ctenophora), and learning the functions of those opsins.

Methods

Data Collection

We searched both NCBI and UniProt using BLAST (Gish and States 1993) with a bait set of five opsin sequences (accession numbers: BAG80696.1; NP_001014890.1; CAA49906.1; O15974.1; P23820.1) and an e-value cutoff of 1e-5. Our first goal was to maximize potential opsins from understudied taxa, so we excluded vertebrates and arthropods from our BLAST search on NCBI and downloaded the top 250 hits per opsin bait. We then searched Uniref90 with the same bait sequences and cutoff value, and downloaded only lophotrochozoan (NCBI taxonomic ID: 1206795) sequences/clusters. We combined all the sequences we recovered from NCBI and Uniref90 with sequences from other publications, which include tardigrades, arthropods, ambulacraria, cubozoan cnidarians and vertebrates (Hering and Mayer 2014; D'Aniello et al. 2015; Davies et al. 2015; Henze and Oakley 2015; Liegertová et al. 2015). To this initial database of published sequences, we added mollusc opsins that we gathered by running Phylogenetically Informed Annotation, PIA, (Speiser et al. 2014) on transcriptomes and NCBI TSAs from two cephalopods, three chitons, five gastropods, and three bivalves.

Data Grooming

Because our initial data collection was permissive, our raw dataset (over 1,600 sequences) contained duplicate sequences as well as a number of nonopsin GPCRs. We used CD-HIT (Li and Godzik 2006; Fu et al. 2012) to cluster together sequences that were >90% similar, allowing us to remove duplicates and highly similar sequences. To remove nonopsin GPCRs, we first ran the dataset through SATé-II (Liu et al. 2012). SATé-II employs FastTree 2 (Price et al. 2010) on an initial MAFFT (Katoh and Standley 2013) alignment before subdividing the alignment into 200 subproblems and realigning with MAFFT. The realigned subproblems are then merged using MUSCLE (Edgar 2004), and a new tree produced by FastTree, and the maximum likelihood (ML) score is calculated. SATé-II iterates until a pre-defined stopping point or likelihood improvement. Next, we used FigTree (Rambaut 2007) to visualize trees, rooted with melatonin receptors (Plachetzki et al. 2010; Feuda et al. 2014). We then trimmed this tree to exclude nonopsins using a custom python script called Supercuts (Swafford 2016) and retained the ingroup clade for subsequent analyses. We removed any sequences from the alignment that lacked the conserved lysine residue homologous to

K296 of bovine rhodopsin. We also manually trimmed the beginning and end of the alignment to the first and last aligned blocks using Aliview (Larsson 2014). Finally, although they lack the conserved lysine, we added the *Trichoplax adherens* placopsins back to our dataset as a close outgroup to root our tree, as Feuda et al. (2012) showed that placopsins are sister to all other animal opsins. In total, our groomed dataset had 768 opsins with the conserved K296 (plus three placozoan opsins without the lysine) from 248 species across 14 phyla.

Tree Estimation and Support Values

To create the final alignment for our dataset, we ran SATé on our dataset using the following configuration: a subproblem fraction of 0.025, stopping iterations after five unimproved ML scores and FastTree under the GTR gamma model. We next used the MPI version of IQ-TREE 1.4.0 (Nguyen et al. 2014) to select a substitution model based on our SATé alignment, infer a maximum likelihood tree, and compute support values. IQ-TREE incorporates an approach for calculating ultrafast bootstraps (UFBoot), which may have fewer biases compared with other bootstrapping methods (Minh et al. 2013). We were also able to perform the SH-like approximate likelihood ratio test (SH-aLRT) and the approximate Bayes test as implemented in IQ-TREE to assess support for single branches to complement our UFBoot analysis (Guindon et al. 2010; Anisimova et al. 2011). SH-aLRT branch supports are often more consistent and conservative than bootstrapping methods (Simmons and Norton 2014; Simmons and Randle 2014). The IQ-TREE substitution model test selected the LG + F+R8 model for our alignment based on BIC. Because we had a large number of relatively short sequences, we performed 50 ML tree searches varying the perturbation value (0.1– 0.5). IQ-TREE keeps the best ML tree while it searches the tree parameter space, and stops searching after going through a user-defined number of trees. We extended this number to 500 trees to better explore tree parameter space. Two trees had virtually identical, high log-likelihood scores, and so we ran IQ-TREE again, setting each tree as the starting tree, to break the tie and to get UFBoot, SH-aLRT and aBayes values for the final, highest log-likelihood tree. The code used for this analysis, our dataset and the resultant tree are available on BitBucket (UCSB Phylogenetics).

Tree Reconciliation and Rearrangement

We used NOTUNG 2.8 (Chen et al. 2000) to reconcile the gene tree with a metazoan species tree based on NCBI Taxonomy. This animal phylogeny places sponges as sister to all other animals, and posits unresolved relationships between ctenophores, cnidarians and bilaterians. While the order of branching in early metazoans is contentious, we do not expect it to affect our estimate of the number of paralogs present in the last common ancestor of

Cnidaria + Bilateria. Because we were unable to include Xenacoelomorpha opsins in our phylogeny, our estimate of bilaterian opsin paralogs applies only to the last common ancestor of protostomes and deuterostomes the Nephrozoa. To perform both a reconciliation and rearrangement of weakly supported branches, NOTUNG requires a fully resolved species tree. We used the ape package (Paradis et al. 2004) in R (R Core Team 2016) to randomly resolve polytomies present in the species tree. Because our analysis focuses on major splits in the animal phylogeny that are well supported, for example protostomes vs deuterostomes, the random resolution of more shallow nodes did not impact our results. We set the penalty for duplications to 1.5, losses to 1.0 and the edge weight threshold for rearrangement to 95.0 (i.e. nodes with <95% UFBoot support are rearranged to minimize duplication and loss costs).

Tree Visualization

We used FigTree 1.4.2 (Rambaut 2007) and TreeGraph2 (Stöver and Müller 2010) to collapse opsin clades by hand according to major taxonomic group (chordates, echinoderms, lophotrochozoans or ecdysozoans), and Evolview (Zhang et al. 2012) to format the tree color and branch length for figure 1. We used iTOL (Letunic and Bork 2011) to combine the tallies of opsins per phylum or molluscan class with animal and mollusc phylogenies (figs. 2 and 3). For supplementary figures S1 and S2, Supplementary Material online, we used ETE3 to build and annotate the trees (Huerta-Cepas et al. 2016). Data and code for these trees are also available at the UCSB Phylogenetics BitBucket. We made final adjustments to the outputs of these programs using OmniGraffle Pro (v. 6.5, Omni Group, Seattle, WA).

Results

From our reconciled tree containing 768 unique sequences, our analysis strongly supports at least nine bilaterian opsin paralogs spread across four eumetazoan paralogs (figs. 1 and 2, complete gene and reconciled gene trees in supplementary figs. S1 and S2, Supplementary Material online). We recover five bilaterian opsin paralog groups described in previous publications: canonical c-opsin, canonical r-opsin, Go-opsin, RGR/retinochrome/peropsin, neuropsin, and "noncanonical r-opsins", which include the formerly described arthropod and lophotrochozoan arthropsins. Our broader taxonomic sampling also allows us to infer three previously undescribed bilaterian paralogs, which we have named "xenopsins", "bathyopsins" and "chaopsins". Because adding so many new bilaterian opsins changes the relationships between paralogs, we establish new, named hypotheses for these relationships, as is often done in species-level phylogenetic analyses (see fig. 1 and table 1). In addition to new clade names, we also use Roman numerals for eumetazoan
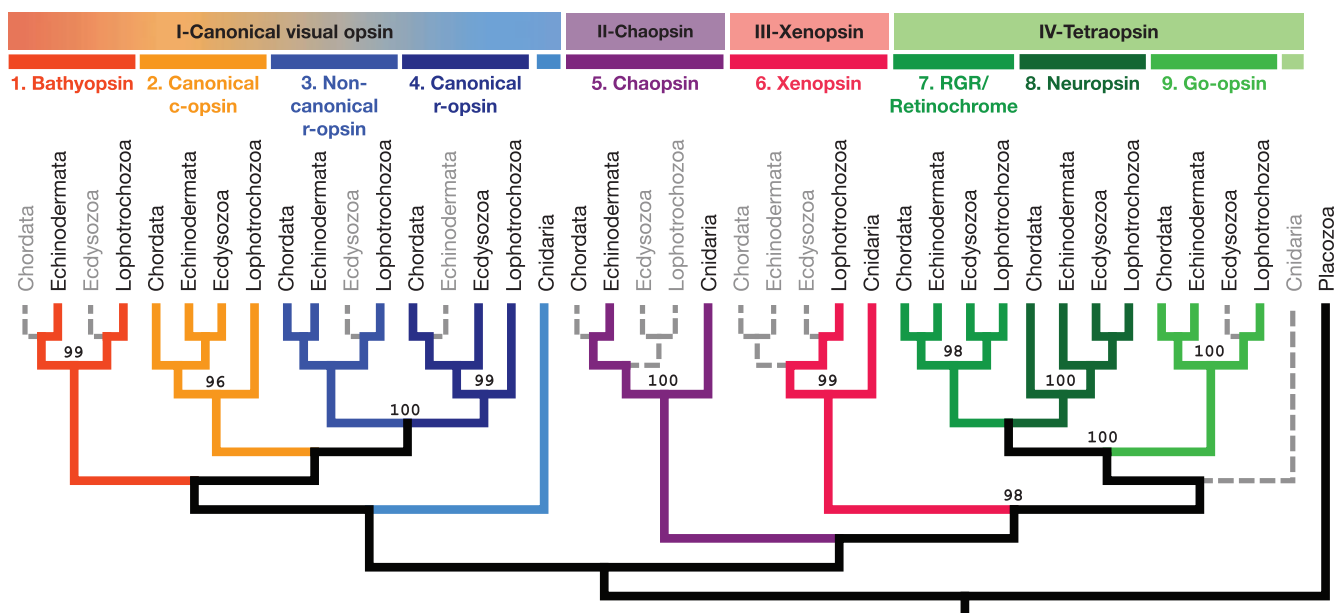

Fig. 1.—There are nine bilaterian opsin paralogs spread among four major eumetazoan opsin paralogs. The four major eumetazoan opsin paralogs are indicated at the top with roman numerals. The nine bilaterian opsin paralogs are indicated with arabic numerals and are color coded to match the corresponding branches. Each opsin clade has been reconciled and collapsed into five major taxonomic groups: chordates, echinoderms, ecdysozoans, lophotrochozoans, and cnidarians. Colored branches indicate the presence of an opsin in at least one species within the major taxonomic group. Light gray dashed branches indicate absence of an opsin paralog from the taxa indicated at the tips. These absences likely represent true losses opsin paralogs. Ultrafast bootstrap (UFBoot) supports from IQ-TREE are given at the nodes they support. All unlabeled nodes had UFBoot supports <95% and were rearranged during tree reconciliation. See supplementary figure S2, Supplementary Material online, for the uncollapsed reconciled tree.
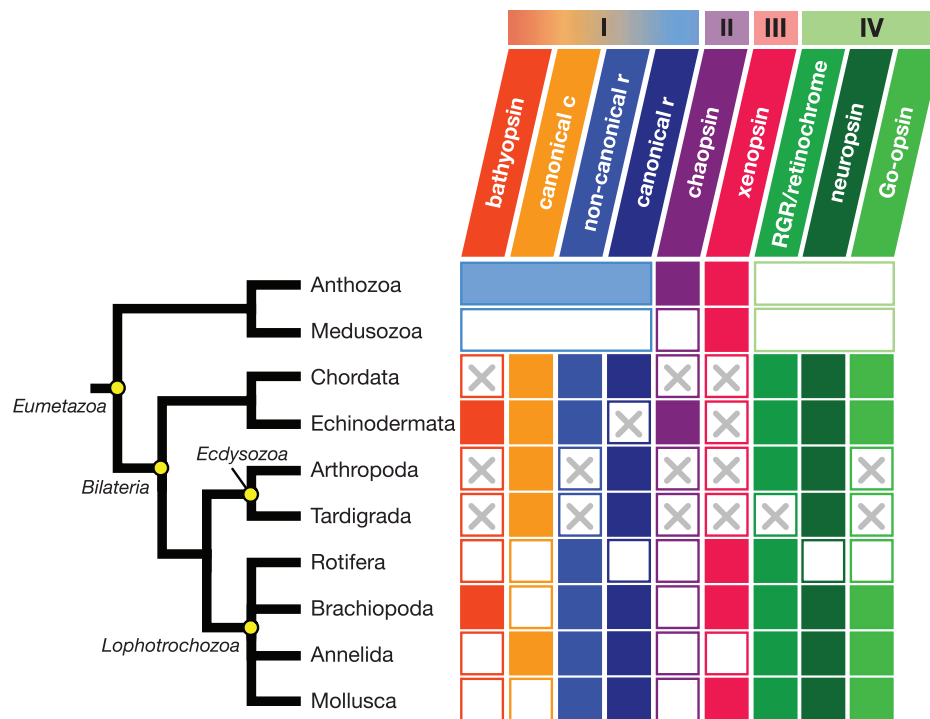
Fig. 2.—The history of opsins is marked by ancient diversity and subsequent losses of paralogs along different animal lineages. Summary of known opsin complements in major animal phyla. Major subdivisions of metazoans are indicated on the phylogeny as yellow dots with italic labels. Phyla are represented at the tips, except for cnidarians, which are broken down into the two major cnidarian splits. Colored bars with roman numerals indicate opsin paralogs present in the most recent ancestor of eumetazoans. The nine bilaterian opsin paralogs are indicated by slanted colored bars and full opsin names. Filled squares represent presence, empty squares absence of at least one sequence from the opsin paralog group for each phylum listed. Gray Xs mark losses of opsins that are strongly supported, based on absence of that opsin paralog in any genomes from the phylum. Note that no extant phylum included in our analysis seems to have the full complement of bilaterian opsins. The maximum is seven opsin paralogs in both echinoderms and brachiopods. The anthozoan I- canonical visual opsin paralog falls sister to bilaterian orthologs, and is indicated by the light blue bar.

paralogs and Arabic numerals for bilaterian paralogs to help clarify which opsin clades are inferred as eumetazoan versus bilaterian paralogs at a glance in the text and figures.

The Last Common Eumetazoan Ancestor Had at Least Four Opsin Paralogs

All cnidarian opsins included in our analysis fell sister to three opsin paralogs also shared by bilaterians: the canonical visual opsins (I), chaopsins (II), and xenopsins (III) (see fig. 1 and supplementary figs. S1 and S2, Supplementary Material online). In our gene tree, Anthozoa II (Hering and Mayer 2014) is sister to the canonical c-opsins, but with mixed support from UFBoot (67) and single branch tests (aLRT = 91.2; aBayes = 0.998). Our reconciliation analysis minimizes duplications and losses, allowing rearrangement of nodes with low UFBoot values, and so places Anthozoa II sister to multiple bilaterian paralogs, including canonical c, noncanonical r, canonical r-opsins, and bathyopsins (fig. 1). However, given the difference in support for the placement of Anthozoa II based on bootstraps, single branch tests, and parsimony, we cannot confidently place these cnidarian

opsins. On the other hand, the cnidarian Anthozoa I (Hering and Mayer 2014) are well supported as sister to echinoderm chaopsins (UFBoot = 100; aLRT = 98.6; aBayes = 1.0). Similarly, the group referred to as cnidops (Plachetzki et al. 2007) are also strongly supported as sister to lophotrochozoan sequences (UFBoot = 99; aLRT = 95.4; aBayes = 1.0), together comprising the xenopsins. Based on the positions of cnidarian opsins, we infer that these three opsin paralogs arose prior to the split of cnidarians + bilaterians, and were thus present in the last common ancestor of eumetazoans. Although we did not find extant cnidarian tetraopsins, we infer from our reconciled tree that the last common eumetazoan ancestor did have a tetraopsin, raising our estimate of eumetazoan opsin paralogs to at least four.

Early Bilaterian Ancestors Had at Least Nine Different Opsin Paralogs

I. Canonical Visual Opsins

This grouping consists of multiple clades of both previously and newly described opsins, encompassing the canonical
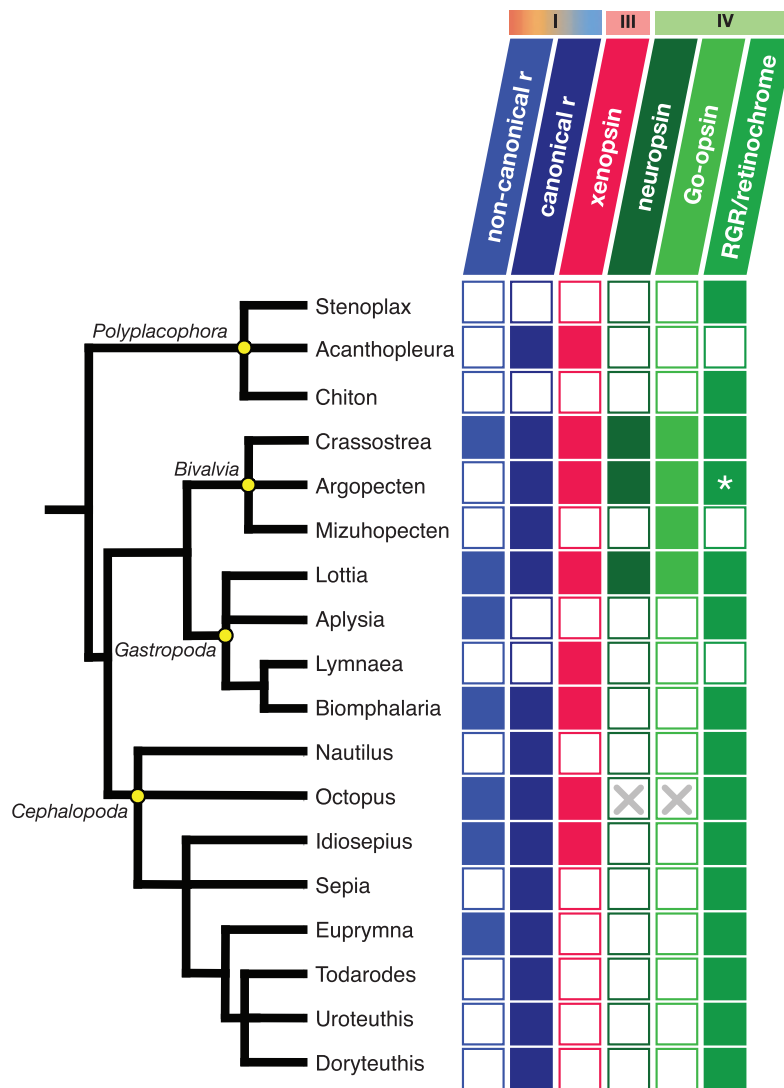
FIG. 3.—The ancestral mollusc likely had seven opsins from six of the bilaterian paralog groups. Summary of known opsin complements within the molluscs. Colored bars with roman numerals indicate opsin paralogs present in the most recent ancestor of eumetazoans. The nine bilaterian opsin paralogs are indicated by slanted colored bars and full opsin names. Filled squares represent presence, empty squares absence of at least one sequence from the opsin paralog for each genus listed. Gray Xs mark losses of opsins that are strongly supported, based on absence of that opsin paralog in the *Octopus bimaculoides* genome. The major classes of molluscs are noted with yellow dots and italic labels. *Argopecten irradians* retinochrome was not included our original analysis, but is present, noted by an asterisk (see supplementary fig. S3, Supplementary Material online, for RGR/retinochrome gene tree that includes this sequence).

visual opsins in both vertebrates and invertebrates. Because the relationships between these clades generally received low UFBoot support, their current placement together comes primarily by our reconciliation analysis.

1. New opsin group: Bathyopsins. The group of opsin paralogs we have named bathyopsins is a small but well supported, monophyletic, bilaterian clade (see figs. 1 & 4, UFBoot = 99). Sequences from the echinoderms, Echinopsins A (D'Aniello et al. 2015), represent deuterostomes, and sequences from the genome of the brachiopod *Lingula* represent prostostomes.

2. Canonical c-opsins. We have renamed as "canonical c-opsins" the monophyletic clade of vertebrate visual and brain c-opsins, arthropod pteropsins (Velarde et al. 2005), and *Platynereis* c-opsin (Arendt et al. 2004). We recovered the canonical c-opsins with high support (UFBoot = 96, see figs. 1 & 4). Despite mining numerous mollusc transcriptomes for opsin sequences, we did not recover any additional lophotrochozoan or protostome c-opsins besides the single c-opsin reported from the annelid *Platynereis dumerilii*.

3. Noncanonical r-opsins. The noncanonical r-opsins are sister to the canonical r-opsins with high support

1. Bathyopsin

5. Chaopsin

2. Canonical c

3. Non-canonical r
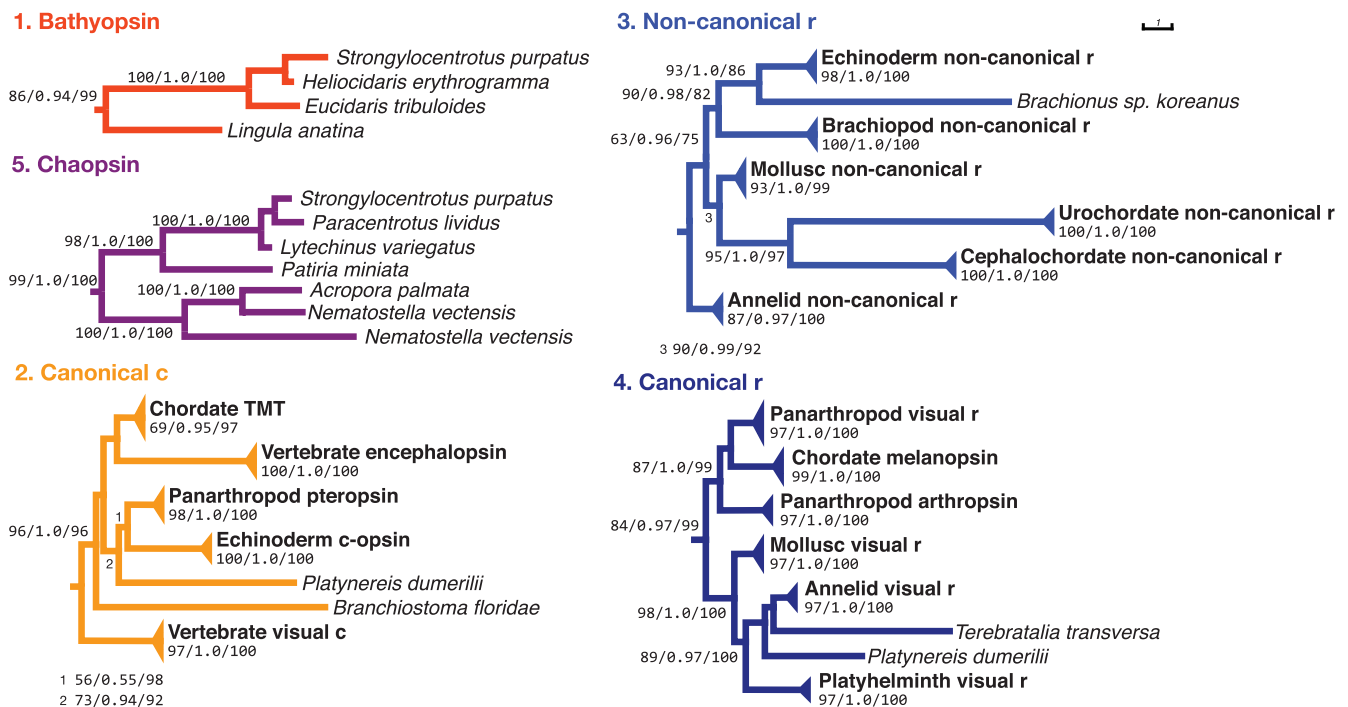

4. Canonical r

Fig. 4.—Opsin paralog trees for the Gq-opsins and C-opsins, representing the relationships between opsin orthologs by phylum. Each tree shows opsin sequences collapsed by clade. Values below the clade name represent SH-aLRT/aBayes/UFBoots. Only clades with bootstrap supports >75% are shown. The full gene tree can be found in supplementary figure S1, Supplementary Material online.

Table 1

Summary of Opsins Present Before Bilaterians and Present in the Last Common Ancestor of Most Bilaterians (excluding Xenoacoelomorpha)

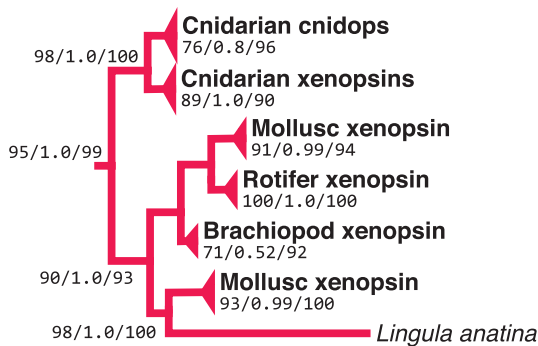| Last common eumetazoan ancestor opsin paralogs	Last common bilaterian ancestor opsin paralogs	Previously named clades within each group	UFBoot support
I. Canonical visual opsins	1. Bathyopsins	echinoderm and inarticulate brachiopod bathyopsins	99
	2. Canonical c-opsins	chordate TMT, chordate encephalopsins, echinoderm encephalopsin-like, arthropod pteropsins, *Platynereis* c-opsin, vertebrate visual c-opsins	96
	3. Noncanonical r-opsins	lophotrochozoa, ambulacrarian and cephalochordate "arthropsins"	**
	4. Canonical r-opsins	lophotrochozoan visual r-opsins, platyhelminthes r-opsin, chordate melanopsins, arthropod visual r-opsins, arthropod arthropsins	99
II. Chaopsins	5. Chaopsins	echinoderm Echinopsins B and Anthozoa I	100
III. Xenopsins	6. Xenopsins	cnidarian cnidops, lophotrochozoan xenopsins	99
IV. Tetraopsins	7. RGR/Peropsins/Retinochromes	chordate Rrh/RGR/peropsin, echinoderm RGR-like, mollusc retinochrome/peropsin-like/arthropod peropsin-like	98
	8. Go-opsins	echinoderm, cephalochordate and lophotrochozoan Go-opsins	100
	9. Neuropsins	chordate, nonmammalian vertebrate, ambulacrarian, lophotrochozoan and arthropod neuropsins/opn5	100

NOTE.— We considered UFBoot values >95 as strong support for the monophyly of that group, but allowed branch rearrangements below that threshold. Asterisks (**) indicate support for the node based on reconciliation with the species tree.

(UFBoot = 100, see fig. 1), though we do not have strong support for the monophyly of the noncanonical r-opsins, even after reconciliation (see figs. 1 and 4 and supplementary fig. S1, Supplementary Material online). The noncanonical r-opsins contain sequences from deuterostome lineages 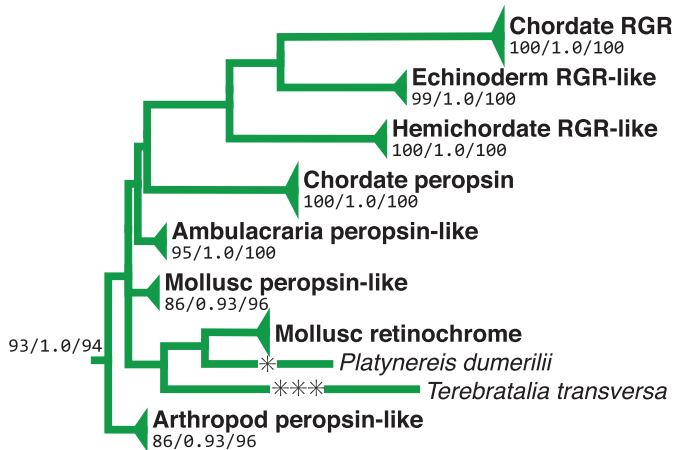like echinoderms, hemichordates and cephalochordates, and previously unannotated sequences from protostomes including annelids, brachiopods and molluscs.

4. Canonical visual r-opsins. This opsin group is well supported (UFBoot = 99, see fig. 1 & 4) and includes the following four clades: the canonical visual opsins of arthropods; the
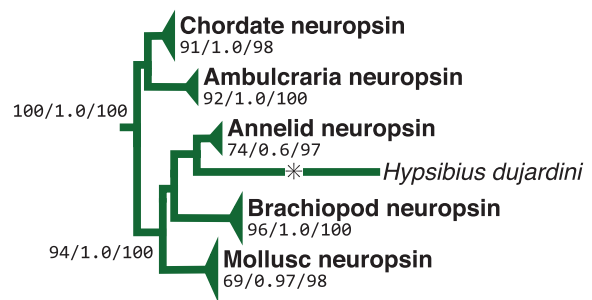
6. Xenopsin

Cnidarian cnidops
76/0.8/96
Cnidarian xenopsins
89/1.0/90
98/1.0/100
95/1.0/99
Mollusc xenopsin
91/0.99/94
Rotifer xenopsin
100/1.0/100
Brachiopod xenopsin
71/0.52/92
90/1.0/93
Mollusc xenopsin
93/0.99/100
98/1.0/100
Lingula anatina

7. RGR/peropsin/retinochrome

Chordate RGR
100/1.0/100
Echinoderm RGR-like
99/1.0/100
Hemichordate RGR-like
100/1.0/100
Chordate peropsin
100/1.0/100
Ambulacraria peropsin-like
95/1.0/100
Mollusc peropsin-like
86/0.93/96
Mollusc retinochrome
* *Platynereis dumerilii*
93/1.0/94
*** *Terebratalia transversa*
Arthropod peropsin-like
86/0.93/96

8. Neuropsin

Chordate neuropsin
91/1.0/98
Ambulcraria neuropsin
92/1.0/100
100/1.0/100
Annelid neuropsin
74/0.6/97
* *Hypsibius dujardini*
Brachiopod neuropsin
96/1.0/100
94/1.0/100
Mollusc neuropsin
69/0.97/98

9. Go-opsin

82/0.99/75
Echinoderm Go
97/1.0/100
Lingula anatina
91/1.0/99
Mollusc Go
Annelid Go
79/0.97/91
98/1.0/100
Argopecten irradians
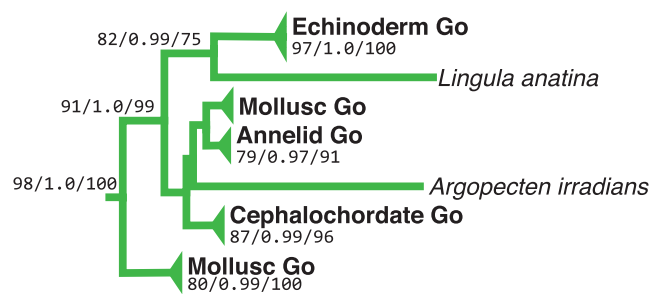**Cephalochordate Go**
87/0.99/96
Mollusc Go
80/0.99/100

Fig. 5.—Opsin paralog trees for the tetraopsins and xenopsins, representing the relationships between opsins by phylum. Each tree shows opsin sequences collapsed by clade. Values below the clade name represent SH-aLRT/aBayes/UFBoots. Only clades with bootstrap supports >75% are shown. The full gene tree can be found in supplementary figure S1, Supplementary Material online. Each asterisk "*" on a branch represents a shortening by five branch length units.

chordate melanopsins and arthropod arthroposins; the canonical visual opsins of mollusks; and the (presumably) visual r-opsins from annelids, brachiopods and platyhelminths.

II. 5. New opsin group: chaopsins

The opsin group we have named chaopsins consists of two previously described clades of opsins, Anthozoa I (Hering and Mayer 2014) and the echinoderm Echinopsins B (D'Aniello et al. 2015). The grouping of these anthozoan and echinoderm sequences as monophyletic chaopsins is well supported (see figs. 1 and 4, UFBoot = 100; aLRT = 98.6; aBayes = 1.0).

III. 6. New opsin group: xenopsins

The opsin group we call xenopsins consists of sequences from a variety of lophotrochozoan protostomes (molluscs, rotifers and brachiopods) and cnidarian cnidops. This clade is well supported in our tree (see figs. 1 and 5, UFBoot = 99; aLRT = 95.4; aBayes = 1.0). We did not find support for any

other protostome (e.g. ecdysozoan) or deuterostome xenopsins. We recovered both the lophotrochozoan xenopsins and cnidarian cnidops with strong support (see supplementary fig. S1, Supplementary Material online). The xenopsins are well supported as sister to the tetraopsins (UFBoot = 98; aLRT = 90.8; aBayes = 1.0, see fig. 1 and supplementary fig. S1, Supplementary Material online)

Many xenopsins were initially described as c-opsin-like in previous analyses, including sequences from the genomes of the molluscs *Crassostrea gigas* and *Lottia gigantea* and *Branchionus* sp. rotifers, and those from gene expression data generated from the larval eyes of articulate brachiopod *Terebratalia transversa*, the optic lobes of *Octopus bimaculoides* and the adult eyes of *Idiosepius paradoxus* (Passamaneck et al. 2011; Albertin et al. 2015; Yoshida et al. 2015). However, we believe that the limited taxonomic scope of previous analyses lead to the incorrect classification of these sequences as c-opsin-like. Our tree is the first to include all of these sequences into a single analysis, and our results clearly support them as a monophyletic clade. Finally,

in addition to xenopsins that were previously described, we found 7 new mollusc xenopsins from combing through transcriptomes (included in fig. 3 and supplementary table S1, Supplementary Material online).

IV. Tetraopsins

Similar to previous analyses (Porter et al. 2012; Feuda et al. 2014; Hering and Mayer 2014), we recover the tetraopsins (IV), formerly "RGR/Go" or "Group 4" opsins, as a monophyletic group with strong support (figs. 1 and 5, UFBoot = 100; aLRT = 98.9; aBayes = 1.0). They consist of RGR/retinochromes/peropsins, Go-opsins, and neuropsins. Because our tree shows strong support for these opsins as most closely related to each other, we have renamed this clade of opsins tetraopsins. Further, we find that each of the previously recognized major clades within tetraopsins has representatives from both protostomes and deuterostomes (see fig. 1).

7. RGR/retinochromes/peropsins.
The RGR/retinochrome/peropsin clade is well-supported by our tree (UFBoot = 98, see fig. 4). Deuterostome RGRs include the original RGRs identified in vertebrates, as well as RGR-like sequences in cephalochordates, hemichordates, and echinoderms (Jiang et al. 1993; Holland et al. 2008; D'Aniello et al. 2015). Deuterostome peropsins include RRH from vertebrates as well as peropsin-like sequences from cephalochordates, hemichordates and echinoderms (Sun et al. 1997; Holland et al. 2008; D'Aniello et al. 2015). Protostome retinochromes include the originally described retinochromes from cephalopods, plus retinochrome-like sequences in bivalve and gastropod molluscs (Hara and Hara 1967; Katagiri et al. 2001). We recovered an additional 3 retinochrome-like sequences from mollusc transcriptomes, including one from the gastropod *Bithynia siamensis goniomphalos* and two from the chitons *Stenoplax conspicua* and *Chiton virgulatus*. In addition to the molluscs, we found retinochrome-like sequences in the brachiopod *Terebratalia transversa*, previously described as a Go-opsin (Passamaneck and Martindale 2013) and a sequence previously described as a peropsin in the annelid *Platynereis dumerilli* (Marlow et al. 2014). We also found a small clade of protostome sequences that fell outside of the protostome retinochromes, including four sequences from the genomes of the mollusks *Crassostrea gigas*, *Lottia gigantea* and *Octopus bimaculoides* (Albertin et al. 2015). Finally, noninsect arthropod peropsin-like sequences (Henze and Oakley 2015) also belonged in the clade of protostome retinochromes. It is unclear from our analysis whether RGR/retinochromes and peropsins are separate bilaterian paralogs. We did recover distinct groups, suggestive of two bilaterian clades, but had low support values at these nodes, and so we collapsed the groups together (see supplementary fig. S1, Supplementary Material online).

8. Neuropsins.
The split between the protostome and deuterostome neuropsins is well supported (UFBoot = 100, see figs. 1 and 5). Deuterostome neuropsins/opn5 sequences include a large clade of vertebrate and cephalochordate neuropsins, a large clade of nonmammalian vertebrate neuropsins, plus neuropsin-like sequences from the Ambulacraria (including those from both hemichordates and echinoderms). Neuropsins from protostomes include sequences from annelids, both *Platynereis dumerilli* (Gühmann et al. 2015) and *Capitella teleta* (Simakov et al. 2012), bivalve and gastropod molluscs, and from the brachiopod *Lingula anatina* (previously annotated as a peropsin). We recovered an additional bivalve neuropsin from the transcriptome of the scallop *Argopecten irradians*. We also found two pan-arthropod neuropsin-like sequences from water flea *Daphnia pulex* (Hering and Mayer 2014; Brandon 2015) and the tardigrade *Hypsibius dujardini* (Hering and Mayer 2014).

9. Go-opsins.
The deuterostome and protostome Go-opsins form a well-supported clade of bilaterian opsins (UFBoot = 100, see figs. 1 and 5). We recovered the same deuterostome Go-opsins from echinoderms and cephalochordates as identified from previous analyses (D'Aniello et al. 2015). From protostomes, we found previously described sequences of Go-opsins from both bivalve and gastropod molluscs, and also sequences from brachiopods and annelids. We also recovered a new Go-opsin from the transcriptome of the scallop *A. irradians*.

Discussion

Reconstructing the evolutionary history of opsins is vital for understanding how light-detecting structures like eyes evolved. Unfortunately, the problem of how and when opsin diversity arose is made difficult by the large number of duplications and losses that have occurred within their evolutionary history. While most analyses of opsin diversity to date have focused on understanding the opsins present within a set of focal taxa (Plachetzki et al. 2007; Feuda et al. 2012, 2014; Hering and Mayer 2014; D'Aniello et al. 2015), we included multiple poorly sampled phyla to ensure the broadest phylogenetic scope to date, for a total of 248 species from 14 phyla. Our analysis reveals three previously unrecognized opsin paralogs in extant animals, and the surprising result that these three additional opsin paralogs likely arose early in the evolution of bilaterians, followed by losses and duplications within those opsins that remained.

Our first major finding is the presence of 9 bilaterian opsin paralogs in extant animals that we infer were also present in the last common ancestor of protostomes and deuterostomes. In addition to the 6 previously identified bilaterian opsins (c-opsin, r-opsin, Go-opsin, peropsin/RGR/retinochrome, neuropsin and noncanonical r-opsin), we propose three additional bilaterian opsins—xenopsins, bathyopsins

and chaopsins. While we acknowledge the need for additional sequence data to confirm the monophyly of these clades of opsin paralogs, our results are consistent with the hypothesis that these opsin paralogs were all present in the last common ancestor of Nephrozoa (protostomes + deuterostomes, excluding Xenacoelomorpha) and potentially bilaterians (depending on the opsins present in Xenacoelomorpha). Hints of the three new opsin groups we identified can be seen in previous opsin phylogenies (Hering and Mayer 2014; D'Aniello et al. 2015), but hypotheses for how these orphaned sequences relate to other better-studied opsins remained obscure with less broad taxonomic coverage.

For example, cnidarian cnidops have been difficult to place consistently within opsin phylogenies. We found that cnidops fall sister to the lophotrochozoan xenopsins with high bootstrap and branch support, suggesting they together form a monophyletic clade. Further, the hypothesis of xenopsins as the sister clade to the tetraopsins is also well supported both by UFBoot and single branch tests. If our reconciled gene tree is correct, the grouping of lophotrochozoan and cnidarian xenopsins suggests that xenopsins were present in both the bilaterian and eumetazoan ancestors. Our result differs from previous studies (Plachetzki et al. 2007; Feuda et al. 2012; Bielecki et al. 2014), because these did not include bilaterian xenopsin-like sequences. Thus, Plachetzki et al. (2007) concluded that cnidops was its own eumetazoan opsin paralog, lost from bilaterians entirely. Both Feuda et al. (2012) and Bielecki et al. (2014) proposed cnidops as sister to the tetraopsins, and inferred that a tetraopsin was present in the eumetazoan ancestor. Our results are consistent with Feuda et al. (2012) and Bielecki et al. (2014), but our inferences differ—instead of the single eumetazoan tetraopsin, we infer two eumetazoan paralogs, xenopsins and tetraopsins.

Lophotrochozoan xenopsins are a well-supported monophyletic clade, suggesting that xenopsins were present in the lophotrochozoan ancestor. Interestingly, xenopsins are absent from publicly available *Platynereis* opsins and the *Capitella* and *Helobdella* genomes. However, because our sampling from annelids is so sparse given the large number of species in the phylum, it seems likely that annelid xenopsins could be uncovered after broader sampling. Xenopsins are also absent from both the ecdysozoan and deuterostome taxa included in our analysis. Given that arthropods, chordates, and echinoderms are now well-sampled for opsin diversity, we hypothesize that the absence of xenopsins these groups reflects true losses of xenopsins from ecdysozoan and deuterostome lineages. Given this hypothesis, we infer that xenopsins were lost at least 3 times in bilaterians: from ancestors of the annelids, Panarthropoda, and the deuterostomes.

Increased taxon sampling also allows us to hypothesize the bathyopsins and chaopsins as paralogs present in the last common ancestor of most bilaterians. These opsins are unusual because of their extreme phylogenetic sparseness, suggesting that if our gene tree inference is correct, these opsin paralogs were lost in the majority of bilaterians. However, we interpret this sparseness as an indication that even our inclusive dataset may still be under-sampling true opsin diversity in animal phyla. Bathyopsins are found in only two phyla so far, Echinodermata and Brachiopoda, forming a well supported, monophyletic clade in our tree. Given that bathyopsins are represented by one deuterostome and one protostome, we infer that bathyopsins were present in the last common bilaterian ancestor. We have not found chordate or hemichordate representatives. In protostomes, we infer that the lophotrochozoan ancestor had bathyopsins, but as bathyopsins are unknown in ecdysozoa entirely, it is possible that they were lost in ecdysozoa after the lophotrochozoan/ecdysozoan split. Because opsins from chordates and arthropods are well sampled, it is unlikely that these phyla possess bathyopsins. We have not uncovered annelid, mollusc or rotifer bathyopsins, yet sparse sampling in these taxa makes it possible that opsin surveys from lophotrochozoans will reveal more bathyopsins in these phyla.

We found chaopsins in only two phyla so far, echinoderms and cnidarians, and their monophyly is supported by both high UFboots and single branch tests. Given our dataset and analysis, we hypothesize that chaopsins were lost at least 3 times in bilaterians: twice from deuterostomes (chordates and hemichordates) and once in the ancestor of all protostomes (including both ecdysozoans and lophotrochozoans). We also find that anthozoans are the only cnidarians that have chaopsins, which suggests another potential loss of chaopsins from the ancestor of hydrozoans and cubozoans. As with the other new opsin types we have described, we are more confident that chaopsins are truly lost from chordates and arthropods compared with the undersampled lophotrochozoans.

Our second major finding is the eumetazoan ancestor likely had at least four opsin paralogs, based on the distribution of cnidarian opsins in our analysis. Instead of inferring eumetazoan c-, r-, and tetraopsins as previously reported (Feuda et al. 2012; Bielecki et al. 2014; Hering and Mayer 2014), we found cnidarian orthologs of the canonical visual opsins, xenopsins and chaopsins. Along with these three eumetazoan opsins, we infer that the last common eumetazoan ancestor also had a tetraopsin, but this paralog is not present in the cnidarians we surveyed. However, because cnidarians are not well sampled, it is possible that a cnidarian ortholog of the bilaterian tetraopsins may be uncovered. Overall, we successfully identified well-supported bilaterian orthologs of at least two cnidarian opsins—cnidops as xenopsins, and Anthozoa II opsins as chaopsins, and infer that the last common ancestor of eumetazoans must have had at least 4 different opsins. Adding more opsins from Cnidaria, Ctenophora, and Xenacoelomorpha may help solidify deeper relationships between well-documented opsin paralogs like the canonical c- and r-opsins and the opsin paralogs we have identified in this analysis.

We used a traditional animal phylogeny to reconcile our gene tree, with ctenophores placed sister to cnidarians, and these two phyla together as sister to bilaterians ("ctenophores-in" hypothesis). This traditional view is recently challenged by multiple studies that instead place ctenophores sister to all other animals ("ctenophores-out" hypothesis) (Dunn et al. 2008; Ryan et al. 2013; Moroz et al. 2014; Borowiec et al. 2015; Pisani et al. 2015; Halanych et al. 2016). There seem to be two opsin paralogs in ctenophores, but the relationship between ctenophore opsins and those from other animals is contentious, particularly the placement of Mnemiopsis 3 (Schnitzler et al. 2012; Feuda et al. 2014). Although Mnemiopsis 3 does have the conserved lysine that aligns at bovine rhodopsin position 296, it was excluded from Hering and Mayer (2014) because it contains an insertion not found in any other opsin. Its placement in the metazoan opsin phylogeny is also highly sensitive to outgroups as seen in Schnitzler et al. (2012) and Feuda et al. (2014). For these reasons, we did not include Mnemiopsis 3 in our analysis. Overall, our estimates of opsin repertoires in the last common eumetazoan ancestor and early bilaterians are likely not greatly impacted by the current controversy about the relationship between ctenophores and other animals (Borowiec et al. 2015; Pisani et al. 2015, 2016; Halanych et al. 2016). "Ctenophores-in" might suggest that they have lost some of the eumetazoan opsin paralogs, whereas "ctenophores-out" suggests a very early origin of the first opsin, and a likely loss of opsins in sponges. At present our results do not distinguish between either ctenophore hypothesis, as the ctenophore opsins we included were not placed in the animal opsin phylogeny with high support.

Opsin evolution is surprisingly complex, hinting at just how much we have yet to learn about how animals use opsins, how these functions shaped the evolution of the gene family, and the physiology and behaviors that require opsins. Besides spatial vision, opsins are used for myriad purposes, for example as depth-gauges or for circadian rhythms (Bennett 1979; Lythgoe 1979; Bybee et al. 2012). Further, opsins are not only expressed in eyes, but also across the bodies of animals (reviewed in Ramirez et al. 2011). It is not yet clear to what extent the loss of an opsin paralog within an animal lineage suggests the concomitant loss of the organismal function, or whether other opsin paralogs can take over that function. At present, we have no functional data for the majority of the 700+ opsins included in this analysis, but current data suggest different animal phyla use related opsins for different purposes. For example, r-opsins likely mediate vision in many protostome eyes, but the orthologous melanopsins in vertebrate retinal ganglion cells only have roles in nonvisual tasks. While opsins are canonical light detectors, two recent studies have shown roles for opsins in both heat sensing and detecting mechanical stimuli in Drosophila (Shen et al. 2011; Senthilan et al. 2012). These studies provide a tantalizing glimpse into opsin functions in sensory modalities besides light detection.

Without understanding the true extent of opsin diversity, we cannot understand opsin evolution, the evolution of eyes and other light sensors, or even how a complex trait like eyes can evolve.

Supplementary Material

Supplementary data are available at *Genome Biology and Evolution* online.

Acknowledgments

Literature Cited

Albertin CB, et al. 2015. The octopus genome and the evolution of cephalopod neural and morphological novelties. Nature 524:220–224.

Anisimova M, Gil M, Dufayard J-F, Dessimoz C, Gascuel O. 2011. Survey of branch support methods demonstrates accuracy, power, and robustness of fast likelihood-based approximation schemes. Syst Biol. 60:685–699.

Arendt D, Tessmar-Raible K, Snyman H, Dorresteijn AW, Wittbrodt J. 2004. Ciliary photoreceptors with a vertebrate-type opsin in an invertebrate brain. Science 306:869–871.

Arendt D, Wittbrodt J. 2001. Reconstructing the eyes of Urbilateria. Philos Trans R Soc Lond B Biol Sci. 356:1545–1563.

Bennett MF. 1979. Extraocular light receptors and circadian rhythms. In: Autrum H, editor. Comparative physiology and evolution of vision in invertebrates. Berlin Heidelberg: Handbook of Sensory Physiology Springer. p. 641–663.

Bielecki J, Zaharoff AK, Leung NY, Garm A, Oakley TH. 2014. Ocular and extraocular expression of opsins in the rhopalium of Tripedalia cystophora (Cnidaria: Cubozoa). PLoS One 9:e98870.

Borowiec ML, Lee EK, Chiu JC, Plachetzki DC. 2015. Extracting phylogenetic signal and accounting for bias in whole-genome data sets supports the Ctenophora as sister to remaining Metazoa. BMC Genomics 16:987.

Brandon CS. 2015. The evolutionary biology of vision in Daphnia. University of South Carolina [cited 2016 May 10]. Available from: http://scholarcommons.sc.edu/etd/3100/?.

Bybee SM, et al. 2012. UV photoreceptors and UV-yellow wing pigments in Heliconius butterflies allow a color signal to serve both mimicry and intraspecific communication. Am Nat. 179:38–51.

Cannon JT, et al. 2016. Xenacoelomorpha is the sister group to Nephrozoa. Nature 530:89–93.

Chen K, Durand D, Farach-Colton M. 2000. NOTUNG: a program for dating gene duplications and optimizing gene family trees. J Comput Biol. 7:429–447.

Colbourne JK, et al. 2011. The ecoresponsive genome of Daphnia pulex. Science 331:555–561.

D'Aniello S, et al. 2015. Opsin evolution in the Ambulacraria. Mar Genomics. 24 Pt 2:177–183.

Davies WIL, et al. 2015. An extended family of novel vertebrate photopigments is widely expressed and displays a diversity of function. Genome Res. 25:1666–1679.

Dunn CW, et al. 2008. Broad phylogenomic sampling improves resolution of the animal tree of life. Nature 452:745–749.

Edgar RC. 2004. MUSCLE: multiple sequence alignment with high accuracy and high throughput. Nucleic Acids Res. 32:1792–1797.

Feuda R, Hamilton SC, McInerney JO, Pisani D. 2012. Metazoan opsin evolution reveals a simple route to animal vision. Proc Natl Acad Sci U S A. 109:18868–18872.

Feuda R, Marletaz F, Bentley MA, Holland PWH. 2016. Conservation, duplication and divergence of five opsin genes in insect evolution. Genome Biol Evol. 8:579–587.

Feuda R, Rota-Stabelli O, Oakley TH, Pisani D. 2014. The comb jelly opsins and the origins of animal phototransduction. Genome Biol Evol. 6:1964–1971.

Fu L, Niu B, Zhu Z, Wu S, Li W. 2012. CD-HIT: accelerated for clustering the next-generation sequencing data. Bioinformatics 28:3150–3152.

Gish W, States DJ. 1993. Identification of protein coding regions by database similarity search. Nat Genet. 3:266–272.

Gühmann M, et al. 2015. Spectral tuning of phototaxis by a go-opsin in the rhabdomeric eyes of platynereis. Curr Biol. 25:2265–2271.

Guindon S, et al. 2010. New algorithms and methods to estimate maximum-likelihood phylogenies: assessing the performance of PhyML 3.0. Syst Biol. 59:307–321.

Halanych KM, Whelan NV, Kocot KM, Kohn AB, Moroz LL. 2016. Miscues misplace sponges. Proc Natl Acad Sci U S A. 113:E946–E947.

Hara T, Hara R. 1967. Rhodopsin and retinochrome in the squid retina. Nature 214:573–575.

Henze MJ, Oakley TH. 2015. The dynamic evolutionary history of pancrustacean eyes and opsins. Integr Comp Biol. 55:830–842.

Hering L, et al. 2012. Opsins in onychophora (velvet worms) suggest a single origin and subsequent diversification of visual pigments in arthropods. Mol Biol Evol. 29:3451–3458.

Hering L, Mayer G. 2014. Analysis of the opsin repertoire in the tardigrade Hypsibius dujardini provides insights into the evolution of opsin genes in panarthropoda. Genome Biol Evol. 6:2380–2391.

Holland LZ, et al. 2008. The amphioxus genome illuminates vertebrate origins and cephalochordate biology. Genome Res. 18:1100–1111.

Huerta-Cepas J, Serra F, Bork P. 2016. ETE 3: reconstruction, analysis, and visualization of phylogenomic data. Mol Biol Evol. 33:1635–1638.

Jiang M, Pandey S, Fong HK. 1993. An opsin homologue in the retina and pigment epithelium. Invest Ophthalmol Vis Sci. 34:3669–3678.

Katagiri N, Terakita A, Shichida Y, Katagiri Y. 2001. Demonstration of a rhodopsin-retinochrome system in the stalk eye of a marine gastropod, Onchidium, by immunohistochemistry. J Comp Neurol. 433:380–389.

Katoh K, Standley DM. 2013. MAFFT multiple sequence alignment software version 7: improvements in performance and usability. Mol Biol Evol. 30:772–780.

Larsson A. 2014. AliView: a fast and lightweight alignment viewer and editor for large datasets. Bioinformatics 30:3276–3278.

Lee YJ, et al. 1994. The Drosophila dgq gene encodes a G alpha protein that mediates phototransduction. Neuron 13:1143–1157.

Letunic I, Bork P. 2011. Interactive Tree Of Life v2: online annotation and display of phylogenetic trees made easy. Nucleic Acids Res. 39:W475–W478.

Li W, Godzik A. 2006. Cd-hit: a fast program for clustering and comparing large sets of protein or nucleotide sequences. Bioinformatics 22:1658–1659.

Liegertová M, et al. 2015. Cubozoan genome illuminates functional diversification of opsins and photoreceptor evolution. Sci Rep. 5:11885.

Liu K, et al. 2012. SATé-II: very fast and accurate simultaneous estimation of multiple sequence alignments and phylogenetic trees. Syst Biol. 61:90–106.

Lythgoe JN. 1979. The ecology of vision/J. N. Lythgoe. Oxford, New York: Clarendon Press; Oxford University Press.

Marlow H, et al. 2014. Larval body patterning and apical organs are conserved in animal evolution. BMC Biol. 12:7.

Mason B, et al. 2012. Evidence for multiple phototransduction pathways in a reef-building coral. PLoS One 7:e50371.

Minh BQ, Nguyen MAT, von Haeseler A. 2013. Ultrafast approximation for phylogenetic bootstrap. Mol Biol Evol. 30:1188–1195.

Moroz LL, et al. 2014. The ctenophore genome and the evolutionary origins of neural systems. Nature 510:109–114.

Nathans J, Hogness DS. 1983. Isolation, sequence analysis, and intron-exon arrangement of the gene encoding bovine rhodopsin. Cell 34:807–814.

Nguyen L-T, L.-. N, Schmidt HA, von Haeseler A, Minh BQ. 2014. IQ-TREE: a fast and effective stochastic algorithm for estimating maximum-likelihood phylogenies. Mol Biol Evol. 32:268–274.

Nilsson D-E. 2005. Photoreceptor evolution: ancient siblings serve different tasks. Curr Biol. 15:R94–R96.

Nilsson D-E. 2013. Eye evolution and its functional basis. Vis Neurosci. 30:5–20.

Oakley TH, Speiser DI. 2015. How complexity originates: the evolution of animal eyes. Annu Rev Ecol Evol Syst. 46:null.

O'Tousa JE, Baehr W, Martin RL, Hirsh J, Pak WL. 1985. The Drosophila ninaE gene encodes an opsin. Cell 40:839–850.

Paradis E, Claude J, Strimmer K. 2004. APE: analyses of phylogenetics and evolution in R language. Bioinformatics 20:289–290.

Passamaneck YJ, Furchheim N, Hejnol A, Martindale MQ, Lüter C. 2011. Ciliary photoreceptors in the cerebral eyes of a protostome larva. Evodevo 2:6.

Passamaneck YJ, Martindale MQ. 2013. Evidence for a phototransduction cascade in an early brachiopod embryo. Integr Comp Biol. 53:17–26.

Pisani D, et al. 2015. Genomic data do not support comb jellies as the sister group to all other animals. Proc Natl Acad Sci U S A. 112:15402–15407.

Pisani D, et al. 2016. Reply to Halanych et al.: ctenophore misplacement is corroborated by independent datasets. Proc Natl Acad Sci U S A. 113:E948–E949.

Plachetzki DC, Degnan BM, Oakley TH. 2007. The origins of novel protein interactions during animal opsin evolution. Snel B, editor. PLoS One 2:e1054.

Plachetzki DC, Fong CR, Oakley TH. 2010. The evolution of phototransduction from an ancestral cyclic nucleotide gated pathway. Proc R Soc B Biol Sci. 277:1963–1969.

Porter ML, et al. 2012. Shedding new light on opsin evolution. Proc R Soc Lond B Biol Sci. 279:3–14.

Price MN, Dehal PS, Arkin AP, Others. 2010. FastTree 2–approximately maximum-likelihood trees for large alignments. PLoS One 5:e9490.

R Core Team. 2016. R: A Language and Environment for Statistical Computing. Vienna, Austria: R Foundation for Statistical Computing. Available from: https://www.R-project.org.

Radu RA, et al. 2008. Retinal pigment epithelium-retinal G protein receptor-opsin mediates light-dependent translocation of all-trans-retinyl esters for synthesis of visual chromophore in retinal pigment epithelial cells. J Biol Chem. 283:19730–19738.

Rambaut A. 2007. FigTree, a graphical viewer of phylogenetic trees. Available from: http://tree.bio.ed.ac.uk/software/figtree.

Ramirez MD, Speiser DI, Pankey MS, Oakley TH. 2011. Understanding the dermal light sense in the context of integrative photoreceptor cell biology. Vis Neurosci. 28:265–279.

Ryan JF, et al. 2013. The genome of the ctenophore Mnemiopsis leidyi and its implications for cell type evolution. Science 342:1242592.

Schnitzler CE, et al. 2012. Genomic organization, evolution, and expression of photoprotein and opsin genes in *Mnemiopsis leidyi*: a new view of ctenophore photocytes. BMC Biol. 10:107.

Senthilan PR, et al. 2012. Drosophila auditory organ genes and genetic hearing defects. Cell 150:1042–1054.

Shen WL, et al. 2011. Function of rhodopsin in temperature discrimination in Drosophila. Science 331:1333–1336.

Simakov O, et al. 2013. Insights into bilaterian evolution from three spiralian genomes. Nature 493:526–531.

Simmons MP, Norton AP. 2014. Divergent maximum-likelihood-branch-support values for polytomies. Mol Phylogenet Evol. 73:87–96.

Simmons MP, Randle CP. 2014. Disparate parametric branch-support values from ambiguous characters. Mol Phylogenet Evol. 78:66–86.

Speiser DI, et al. 2014. Using phylogenetically-informed annotation (PIA) to search for light-interacting genes in transcriptomes from non-model organisms. BMC Bioinformatics 15:350.

Stöver BC, Müller KF. 2010. TreeGraph 2: combining and visualizing evidence from different phylogenetic analyses. BMC Bioinformatics 11:7.

Suga H, Schmid V, Gehring WJ. 2008. Evolution and functional diversity of jellyfish opsins. Curr Biol. 18:51–55.

Sun H, Gilbert DJ, Copeland NG, Jenkins NA, Nathans J. 1997. Peropsin, a novel visual pigment-like protein located in the apical microvilli of the retinal pigment epithelium. Proc Natl Acad Sci U S A. 94:9893–9898.

Swafford A. 2016. Supercuts [cited 2016 April 28]. Available from: https://bitbucket.org/swafford/supercuts.

Terakita A. 2005. The opsins. Genome Biol. 6:213.

Velarde RA, Sauer CD, O, Walden KK, Fahrbach SE, Robertson HM. 2005. Pteropsin: a vertebrate-like non-visual opsin expressed in the honey bee brain. Insect Biochem Mol Biol. 35:1367–1377.

Vopalensky P, Kozmik Z. 2009. Eye evolution: common use and independent recruitment of genetic components. Philos Trans R Soc Lond B Biol Sci. 364:2819–2832.

Yoshida MA, et al. 2015. Molecular evidence for convergence and parallelism in evolution of complex brains of cephalopod molluscs: insights from visual systems. Integr Comp Biol. 55:1070–1083.

Zhang H, Gao S, Lercher MJ, Hu S, Chen W-H. 2012. EvolView, an online tool for visualizing, annotating and managing phylogenetic trees. Nucleic Acids Res. 40:W569–W572.

Associate editor: Davide Pisani